Constraints on nuclear parton distribution functions with dijets in pp, pPb collisions at $\sqrt{s_{NN}} = 5.02$ TeV with the CMS detector

Yeonju Go[*] **on behalf of the CMS Collaboration**
Korea University, 145 Anam-ro, Seonbuk-gu, Seoul, Republic of Korea
E-mail: ygo@cern.ch

Dijet measurements in pPb collisions have been shown to be one of the most important tools for constraining the gluon nuclear parton distribution functions (nPDFs) at large Bjorken x. The dijet pseudorapidity distributions are measured as a function of dijet average transverse momentum in order to study the nuclear modifications of PDFs at various factorization scales. The final results from pp and pPb data samples are compared with next-to-leading-order perturbative QCD predictions obtained from both nucleon and nuclear PDFs. In this paper, we show the latest constraints on nPDFs from studies of dijet pseudo-rapidity distributions in pp and pPb collisions with the CMS detector.

---

[*]Speaker.

1. Introduction

The study of the nuclear modifications of the parton distribution functions (nPDFs) plays a crucial role in extracting the properties of the quark-gluon plasma (QGP), a deconfined state of quarks and gluons expected by quantum chromodynamics (QCD), in relativistic heavy ion collisions. The dijet pseudorapidity [$\eta_{\mathrm{dijet}} = (\eta_1 + \eta_2)/2$], where η_i are single jet rapidities, is a useful observable of the gluon nPDF thanks to its small experimental and theoretical uncertainties [1].

In this proceeding we present measurements of dijet production in pPb and pp collisions at $\sqrt{s_{NN}}$ = 5.02 TeV recorded with the CMS detector and corresponding to integrated luminosities of 35 ± 1 nb^{-1} and 27.4 ± 0.6 pb^{-1}, respectively. The dijet pseudorapidity is studied in bins of dijet average transverse momentum [$p_{\mathrm{T}}^{\mathrm{ave}} = (p_{\mathrm{T},1} + p_{\mathrm{T},2})/2 \sim Q$] and compared with next-to-leading order (NLO) pQCD calculations involving different momentum transfer (Q^2) values to provide strong constraints on the nPDF over a wide Bjorken x and Q^2 phase space.

2. Analysis and Results

Jet reconstruction is performed using the CMS particle-flow (PF) algorithm [2] with anti-k_{T} sequential recombination algorithm [3, 4]. Jets are detected in pseudorapidity in the laboratory frame $|\eta_{\mathrm{lab}}| < 3.0$ in the pPb collisions while $-3.465 < |\eta_{\mathrm{lab}}| < 2.535$ in pp collisions. Due to the asymmetric energies of the proton (4 TeV) and lead (1.58 TeV per nucleon) beams in pPb collisions, the nucleon-nucleon center-of-mass frame is boosted by 0.465 in the detector frame. Therefore, η_{dijet} for pp data is shifted by +0.465 to obtain the same pseudorapidity range in the center-of-mass frame. A detailed description of the CMS experiment can be found in Ref. [5].

The correlations between x, η_{dijet} and $p_{\mathrm{T}}^{\mathrm{ave}}$ were studied using the PYTHIA event generator [6] as shown in Fig. 1. Since η_{dijet} and x are highly correlated and Q is controlled by $p_{\mathrm{T}}^{\mathrm{ave}}$, the sensitivity of the dijet system makes a x and Q dependent measurement of nPDFs.
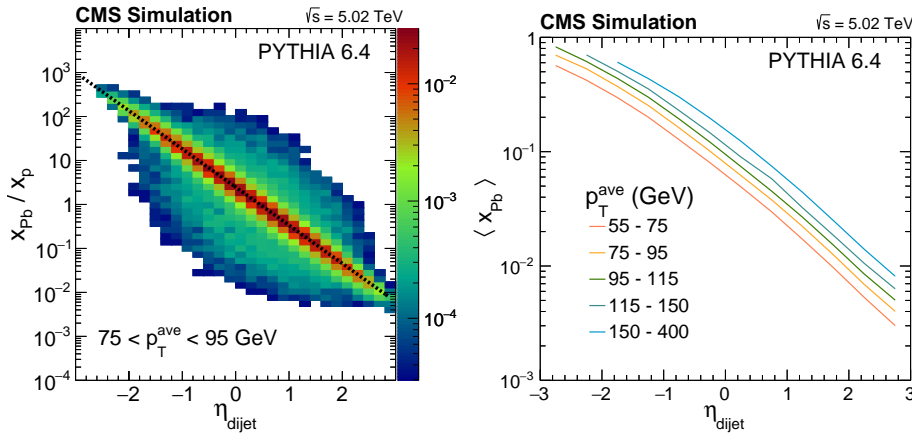
Figure 1: Left: Correlation between the ratio of x_{Pb} and x_{p} and η_{dijet}. Right: Mean x values obtained from particle-level PYTHIA simulations are shown as a function of η^{dijet} in bins of dijet $p_{\mathrm{T}}^{\mathrm{ave}}$. [7]

The η_{dijet} distributions are also measured in pPb collisions and compared to different NLO pQCD predictions using DSSZ, EPS09, and nCTEQ15 nPDFs for various $p_{\mathrm{T}}^{\mathrm{ave}}$ intervals as shown in

Fig. 2. The predicted η_{dijet} distributions from NLO calculations using different nPDF sets are wider than seen in the pPb data. In this comparison, we note that an underlying data-theory discrepancy is already present in pp. The comparisons between pp data and PDF sets can be found in Ref. [7].
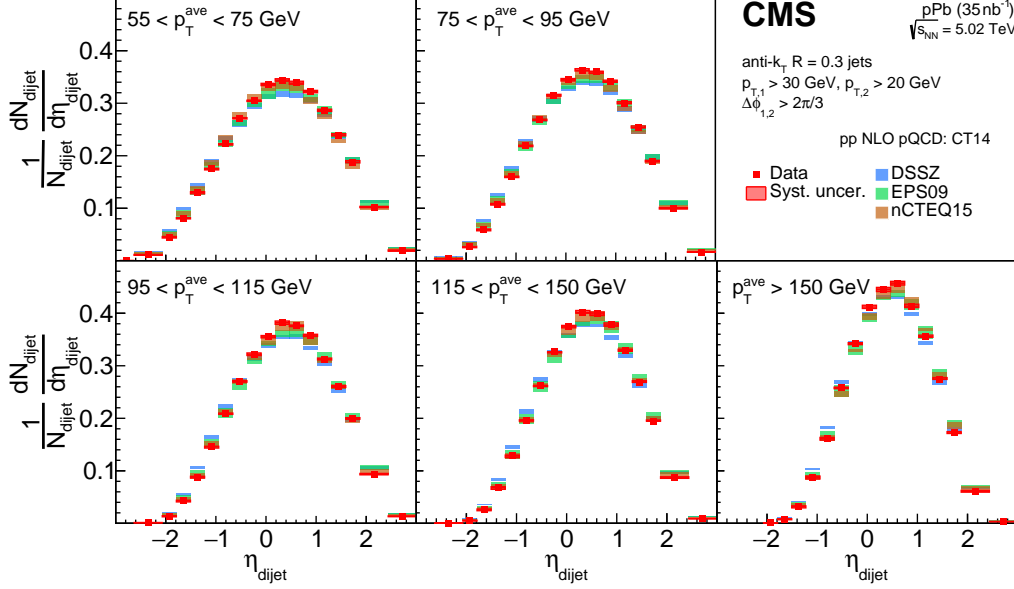
Figure 2: The measured pPb dijet pseudorapidity spectra in bins of dijet average transverse momentum overlaid with NLO calculations for nPDF sets (DSSZ, EPS09 and nCTEQ15) with the CT14 baseline PDF. [7]

Figure 3 shows the ratio of η_{dijet} between pPb and pp in different p_T^{ave} bins. The measurements are compared to the ratios of NLO calculations with variety of nPDFs (DSSZ [8], EPS09 [9] and nCTEQ15 [10] NLO nPDFs with a baseline of CT14 [12] proton PDF) and the calculations with CT14 proton PDF. The ratios of pPb and pp data are seen to deviate significantly from unity in the small and large η_{dijet} regions. One can identify the shadowing at $\eta_{\text{dijet}} > 1.5$, anti-shadowing at $-0.5 < \eta_{\text{dijet}} < 1.5$, and EMC effects at $\eta_{\text{dijet}} < -0.5$. NLO pQCD calculations with EPS09 nPDF match the data at the edge of the theoretical uncertainty in the negative η_{dijet} region, which is sensitive to the gluon EMC effect, while the calculations with DSSZ nPDF, where no gluon EMC effect is present in the global fit, overpredict the data.

The ratio data (pPb/pp) to theory (nPDF/PDF) for various NLO pQCD calculations (DSSZ, EPS09, nCTEQ15, and EPPS16 nPDFs, using CT14 as the baseline PDF) for $115 < p_T^{\text{ave}} < 150$ GeV are shown in Fig. 4. A χ^2 test has been performed to compare the data to theory distributions in the $\eta_{\text{dijet}} < -1$ region, taking into account the point-to-point correlations from nPDFs. For $115 < p_T^{\text{ave}} < 150$ GeV, the p-values from the χ^2 test are 0.19, $< 10^{-8}$, and $< 10^{-8}$ for the EPS09, DSSZ, and nCTEQ15 nPDFs, respectively. For the full p_T^{ave} range, the p values for EPS09 range from 0.19 to 0.95, while the p values for the DSSZ and nCTEQ15 nPDFs are less than 0.015. This shows that, with a p-value cutoff of 0.05, the data are more compatible with the EPS09 nPDFs than with the DSSZ and nCTEQ15 nPDFs. The EPPS16 used these data for the NLO pQCD calculations of its global fit [11].
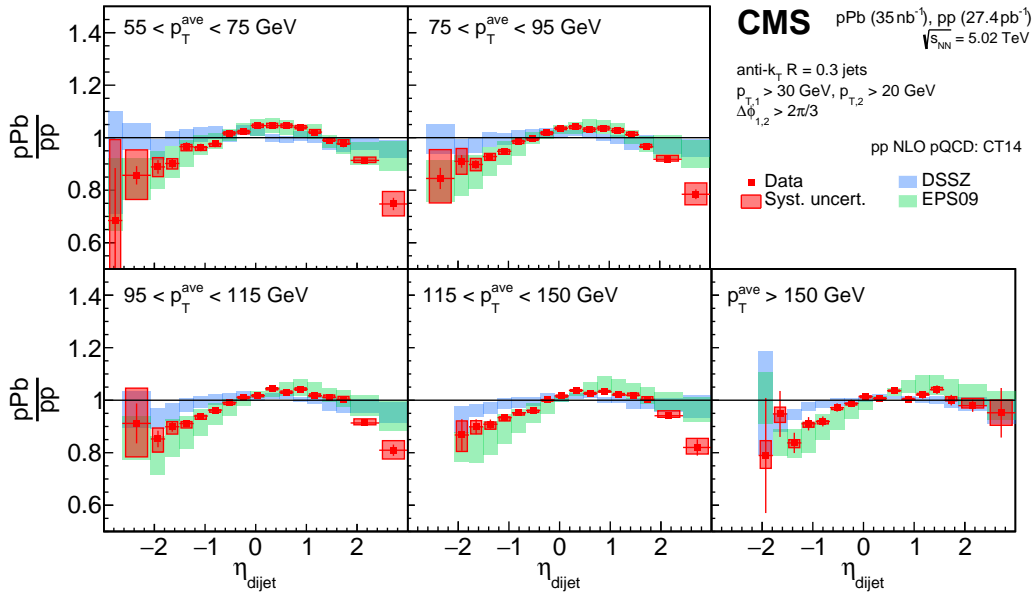
Figure 3: Ratio between pPb and pp dijet pseudorapidity distributions in data and in NLO pQCD calculations. The DSSZ and EPS09 nPDF sets use CT14 as the baseline nucleon PDF. Red boxes indicate systematic uncertainties in data and the height of the NLO pQCD calculation boxes indicates the nPDF uncertainties. [7]
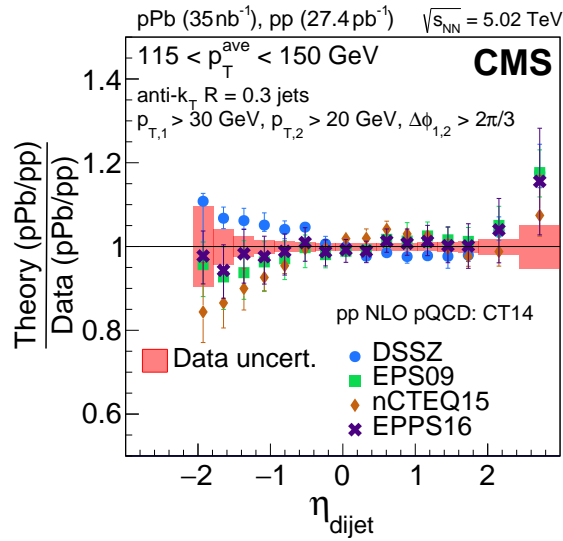
Figure 4: Ratio of theory to data, for the ratio of the pPb to pp η^{dijet} spectra for $115 < p_T^{\mathrm{ave}} < 150$ GeV. Theory points are from the NLO pQCD calculations of DSSZ [8], EPS09 [9], nCTEQ15 [10], and EPPS16 [11] nPDFs, using CT14 [12] as the baseline PDF. Red boxes indicate the total (statistical and systematic) uncertainties in data, and the error bars on the points represent the nPDF uncertainties. [7]

3. Summary

The precision measurements of dijet pseudorapidity (η_{dijet}) in different average transverse mo-

mentum ($p_\mathrm{T}^\mathrm{ave}$) intervals in pPb and pp collisions at a nucleon-nucleon center-of-mass energy $\sqrt{s_{NN}}$ = 5.02 TeV have been reported. The ratio of η_dijet between pPb and pp collisions has been compared to predictions from various NLO pQCD calculations using the DSSZ, EPS09, and nCTEQ15 nPDFs with CT14 as the baseline PDF. Significant modifications of the η_dijet distributions are observed in pPb data compared to the pp reference in all $p_\mathrm{T}^\mathrm{ave}$ intervals, confirming the presence of shadowing, anti-shadowing, and EMC effects in nuclear parton distribution functions. Based on a statistical analysis, the EPS09 nPDF provides the best overall agreement with the data. These data provide strong constraints on the gluon nPDFs [11].

References

[1] K. J. Eskola, H. Paukkunen, and C. A. Salgado, *A perturbative QCD study of dijets in p-Pb collisions at the LHC*, J. High Energy Phys. 10 (2013) 213.

[2] CMS Collaboration, *Particle-flow reconstruction and global event description with the CMS detector*, J. Instrum. 12, P10003 (2017).

[3] M. Cacciari, G. P. Salam, and G. Soyez, *The anti-k_T jet clustering algorithm*, J. High Energy Phys. 04 (2008) 063.

[4] M. Cacciari, G.P. Salam, and G. Soyez, *FASTJET user manual*, Eur. Phys. J. C 72, 1896 (2012).

[5] CMS Collaboration, *The CMS Experiment at the CERN, LHC*, J. Instrum. 3, S08004 (2008).

[6] T. Sjöstrand, S. Mrenna, and P. Skands, *PYTHIA 6.4 physics and manual*, J. High Energy Phys. 05 (2006) 026.

[7] CMS Collaboration, *Constraining gluon distributions in nuclei using dijets in proton-proton and proton-lead collisions at $\sqrt{s_{NN}}$ = 5.02 TeV*, Phys. Rev. Lett. 121, 062002 (2018).

[8] D. de Florian, R. Sassot, P. Zurita, and M. Stratmann, *Global analysis of nuclear parton distributions*, Phys. Rev. D 85, 074028 (2012).

[9] K. J. Eskola, H. Paukkunen, and C. A. Salgado, *EPS09: A new generation of NLO and LO nuclear parton distribution functions*, J. High Energy Phys. 04 (2009) 065.

[10] K. Kovařík, A. Kusina, T. Ježo, D. B. Clark, C. Keppel, F. Lyonnet, J. G. Morfín, F. I. Olness, J. F. Owens, I. Schienbein, J. Y. Yu, *nCTEQ15: Global analysis of nuclear parton distributions with uncertainties in the CTEQ framework*, Phys. Rev. D 93, 085037 (2016).

[11] K. J. Eskola, P. Paakkinen, H. Paukkunen, and C. A. Salgado, *EPPS16: Nuclear parton distributions with LHC data*, Eur. Phys. J. C 77, 163 (2017).

[12] S. Dulat, T.-J. Hou, J. Gao, M. Guzzi, J. Huston, P. Nadolsky, J. Pumplin, C. Schmidt, D. Stump, and C.P. Yuan, *New parton distribution functions from a global analysis of quantum chromodynamics*, Phys. Rev. D 93, 033006 (2016).